processes

MDPI

Article

Selective Complexation and Leaching of Cobalt Using Histidine in an Alkaline Medium

Mengying Li [1,†], Qingliang Wang [1,†], Weiduo Guo [2], Xu Zhao [1], Yaolong Zhang [1], Xiankun Zhou [1], Zhiwu Lei [1,*] and Yahui Zhang [3,*]

[1] School of Resource & Environment and Safety Engineering, University of South China, Hengyang 421001, China
[2] Shanghai Xingzhi High School, Shanghai 201900, China
[3] Faculty of Engineering and Applied Science, Memorial University of Newfoundland, St John's, NL A1B 3X5, Canada
* Correspondence: lzw_1407@usc.edu.cn (Z.L.); yahuizhangcan@gmail.com (Y.Z.)
† These authors contributed equally to this work.

Abstract: Considering the issues of significant ammonia volatilization loss and toxic gas emission associated with the conventional ammonia leaching method used in the resource utilization of cobalt-rich alloy slag, a novel approach involving selective complexation leaching of cobalt in an alkaline histidine solution has been proposed. Under conditions of 35 °C temperature, a molar ratio of histidine to cobalt of 1.5, pH of 8, a leaching period of 12 h, and a stirring speed of 300 rpm, the cobalt leaching rate from cobalt-rich alloy slag exceeds 95%. In contrast, the leaching rates for impurity metals such as iron, lead, and copper remain below 3%, demonstrating outstanding leaching selectivity. Leaching kinetics calculations indicate that the rate-controlling step is chemical reaction control, with an apparent activation energy of 64.32 kJ/mol. Through the use of FTIR and XPS characterization techniques, it has been confirmed that histidine molecules form a stable complex with cobalt ions via the dual coordination of the carboxyl (COO^-) and amino ($-NH_2$) groups. This distinctive bifunctional synergistic coordination mechanism markedly enhances leaching selectivity and reaction efficiency.

Keywords: cobalt; leaching; histidine; cobalt-rich alloy slag

check for updates

Academic Editor: Anna Wołowicz

Received: 23 February 2025
Revised: 21 March 2025
Accepted: 28 March 2025
Published: 31 March 2025

Citation: Li, M.; Wang, Q.; Guo, W.; Zhao, X.; Zhang, Y.; Zhou, X.; Lei, Z.; Zhang, Y. Selective Complexation and Leaching of Cobalt Using Histidine in an Alkaline Medium. *Processes* **2025**, *13*, 1039. https://doi.org/10.3390/pr13041039

Copyright: © 2025 by the authors. Licensee MDPI, Basel, Switzerland. This article is an open access article distributed under the terms and conditions of the Creative Commons Attribution (CC BY) license (https://creativecommons.org/licenses/by/4.0/).

1. Introduction

Co is a critical raw material, and it has been used extensively in the production of batteries, alloys, catalysts, ceramics, and other materials due to its special properties, which include ferromagnetism, corrosion resistance, and temperature-dependent crystal structure [1]. The lower grade of cobalt ores and the increased demand for cobalt have stimulated the development of methods for recovering Co from low-grade metallurgical waste resources. Cu-Co alloy slag is obtained from converter slag, which is reduced by electric furnace and water-quenched. The grade of cobalt in the alloy slag is much higher than that in the ore. Currently, the main methods for processing Co ore include hydrometallurgical and pyrometallurgical approaches [2–5]. Compared to pyrometallurgical processes, hydrometallurgical processes have demonstrated higher metal recovery efficiency, achieving both high product purity and substantial energy savings [6]. At present, the hydrometallurgical methods for extracting Co from cobalt ores involve acid leaching [7], alkaline leaching [8], and bioleaching [9]. In acid leaching processes, HCl, H_2SO_4, HNO_3, and other strong acid solutions are used as leaching agents, and harmful gases such as Cl_2, SO_3,

or NO_x are released. The residual acids after leaching have a significant impact on the environment, which cannot be ignored [10].The ammonia leaching process has always been an effective method for extracting metals from minerals [11]. However, from an operational perspective, the volatile characteristics of ammonia lead to environmental and health risks. High concentrations of ammonia have been maintained throughout the leaching process, resulting in significant ammonia losses. Additionally, ammonia is explosive under high temperatures and pressure [12]. Amino acids (such as glycine) have been proven to be environmentally friendly and effective reagents, capable of selectively leaching various metals from a range of minerals under alkaline conditions [13]. Therefore, replacing ammonia with amino acids as leaching agents for metal recovery may be a better choice.

Eksteen and Oraby [14] were the first to propose the leaching of Cu and Au with glycine. Chen et al. [15] used glycine to leach Co and Li from spent lithium-ion batteries. The highest extractions of 97.07% for Co and 90.95% for Li were achieved at glycine concentration of 300 g/L, 10% H_2O_2, solid-to-liquid molar ratio of 1:100, temperature of 80 °C, and leaching time of 7 h. Manivanna et al. [16] achieved the cobalt leaching recovery of 89.7% from Li^+ batteries (LiBs) using glycine at 100 °C, a slurry concentration of 13.8 g/L, and a glycine concentration of 1.24 mol/L. Eksteen et al. [17] employed an alkaline glycine leaching system to selectively extract Ni and Co successively from serpentine-rich low-grade sulfide ores. It was shown that Ni and Co could be selectively leached using glycine, but the leaching rate was very slow, with 83.5% of nickel and 76.3% of cobalt being leached in 672 h. The effectiveness of glycine-based metal recovery solutions was further validated using multiple technologies, including solvent extraction, sulfide precipitation, carbon adsorption, ion exchange, and chemical reduction [18]. The recyclability of glycine was confirmed by Eksteen and Oraby, particularly in multi-stage extraction systems and reused lean solutions. Although glycine has achieved significant breakthroughs in the leaching of precious metals, its large-scale application remains constrained by critical challenges, such as slow leaching kinetics and insufficient cost-effectiveness of amino acid reagents. The metal complexation efficacy of amino acids is directly governed by the structural configuration and electronic properties of their coordination groups. For instance, histidine, with its polydentate coordination structure—featuring an imidazole ring (π-electron donor), an amino group, and a carboxyl group, exhibits synergistic effects that enable the formation of highly stable cobalt complexes. This demonstrates superior coordination selectivity and leaching kinetics compared to conventional monodentate amino acids.

Histidine (His) is also a naturally basic amino acid, which contains an amino group (NH_2), a carboxyl group (-COOH), and an imidazole ring (1H-imidazole). Various molecular forms were exhibited by it at different pH values [19]. The isoelectric point (pI) of histidine is 7.59. It is polar, easily dissociable and hydrophilic, and is the only amino acid that is buffered at near neutral pH [20]. Metal-amino acid complexes with cyclic structures were formed by the amino and carboxyl groups of amino acids and metal ions in a certain ratio [21]. In contrast, glycine lacks such a buffering group, requiring stricter pH control (pH 10–12) for effective leaching. Currently, histidine has been successfully applied as a ligand in the synthesis of many metal nanoparticles, such as gold [22], silver [23], copper [24], etc. The leaching of gold was promoted by Eksteen and Oraby [25] with an amino acid mixture (glycine and histidine) under conditions of 0.1 mol/L amino acid, 1% H_2O_2, pH 11, and 60 °C. In this study, pure metal cobalt powder was first used as the research object to investigate the reaction mechanism of cobalt leaching with histidine. After systematically studying the influence of key leaching parameters, such as leaching temperature, reagent concentration, stirring speed, histidine/Co molar ratio, and pH, a series of characterization techniques were adopted. The leaching kinetics model of histidine on pure metal cobalt powder was established to further analyze the leaching mechanism of cobalt with histi-

dine. Finally, Cu-Co alloy slag was used to verify the selective leaching effect of histidine on cobalt.

2. Materials and Methods

2.1. Materials

The chemical reagents used in the experiment, including lysine ($C_6H_{14}N_2O_2$), histidine ($C_6H_9N_3O_2$), glycine ($C_2H_5NO_2$), arginine ($C_6H_{14}N_4O_2$), citrulline ($C_6H_{13}N_3O_3$), theanine ($C_7H_{14}N_2O_3$), sulfuric acid (H_2SO_4), and sodium hydroxide (NaOH), were analytically pure reagents, purchased from Sinopharm Chemical Reagent Co., Ltd. (Shanghai, China). The cobalt used in the experiment is 99.99% cobalt powder with a particle size of 90% –200 mesh. The Cu-Co alloy slag sample was obtained from the converter slag during the copper smelting process through reduction smelting and water quenching. Detailed chemical composition of the alloy is listed in Table 1. All analytical samples were prepared with deionized water.

Table 1. Chemical composition of the Cu-Co alloy slag.

Elements	Co	Cu	Fe	Pb	Ni
Wt.%	6.2	30.7	61.2	1.4	0.42

2.2. Leaching Experiment

A total of 1 g of cobalt powder was added to a certain volume of amino acid solution at different amino acid concentrations, leaching temperature, stirring speed, and leaching time. The pH of the solution was adjusted from 7 to 12 using 1% NaOH solution. After leaching, solid–liquid separation was conducted by filtration. The filter cake was dried at 105 °C for 3 h and weighed. The concentration of cobalt ions in the filtrate was analyzed using a flame atomic absorption spectrometer. The initial conditions were set as 0.3 mol/L amino acid concentration, temperature 25 °C, and 12 h leaching time.

A total of 10 g of Cu-Co alloy slag sample was used for leaching at an initial pH of 8, a temperature of 35 °C, a histidine concentration of 0.1 mol/L, and a histidine/Co molar ratio of 1.5:1. The mixtures were then stirred continuously for 6 to 24 h. Samples were extracted periodically to determine the ion concentrations of Co, Cu, Pb, and Fe. After the leaching process was completed, the residue was filtered, then dried at 105 °C for 3 h. The residual metals content in the filter slag were analyzed. The leaching rates of Co, Cu, Pb, and Fe were calculated.

2.3. Analytical Method

The chemical environment and valence state alterations of elements throughout the leaching process were analyzed using X-ray photoelectron spectroscopy (XPS Thermo Fisher Scientific, Waltham, MA, USA). The surface morphology of the leaching residue was scrutinized with a scanning electron microscope (SEM-EDS Regulus 8100, Chiyoda, Japan), while the functional group bonding changes of the amino acids before and after the leaching reaction were analyzed using Fourier transform infrared spectroscopy (FT-IR NEXUS 670, Nicolet, Stafford, TX, USA). The concentration of metal ions was quantified employing a flame atomic absorption spectrometer (AAS, 55B AA, Agilent Technologies Inc., Santa Clara, CA, USA), and the leaching rate of cobalt was computed as per Formula (1).

$$X_{Me} = \frac{C_{Me} \times V}{m \times \omega_{Me}} \times 100\% \quad (1)$$

where X_{Me} is the leaching rate of cobalt, %; C_{Me} is the concentration of cobalt determined by flame atomic absorption spectrometry, mg/L; V is the volume of the filtered leaching

solution, L; m is the mass of cobalt powder, mg; and ω_{Me} is the mass fraction of cobalt (purity), %.

3. Results and Discussion

3.1. Comparison of the Leaching Effects of Different Amino Acids on Cobalt

The effects of four different amino acids with varying numbers and positions of amino groups on cobalt leaching were studied, including glycine (Gly), histidine (His), lysine (Lys), and citrulline (Cit).

The structure of amino acids is influenced by pH, because their charge distribution and intermolecular interactions vary at different pH conditions. The results in Figure 1a demonstrate that histidine, lysine, and arginine all show good leaching effects on cobalt in the pH range of 7 to 10, while the leaching efficiency of cobalt from glycine increased with increasing pH. At pH 11, the leaching rates of histidine and lysine exceeded 95%, while the leaching efficiencies of arginine and glycine decreased to below 90%. At pH 12, the leaching efficiencies of the four amino acids on cobalt significantly declined. As a result, in subsequent experiments, the pH for glycine was set at 10, whereas the pH for the remaining three amino acids was set at 8.

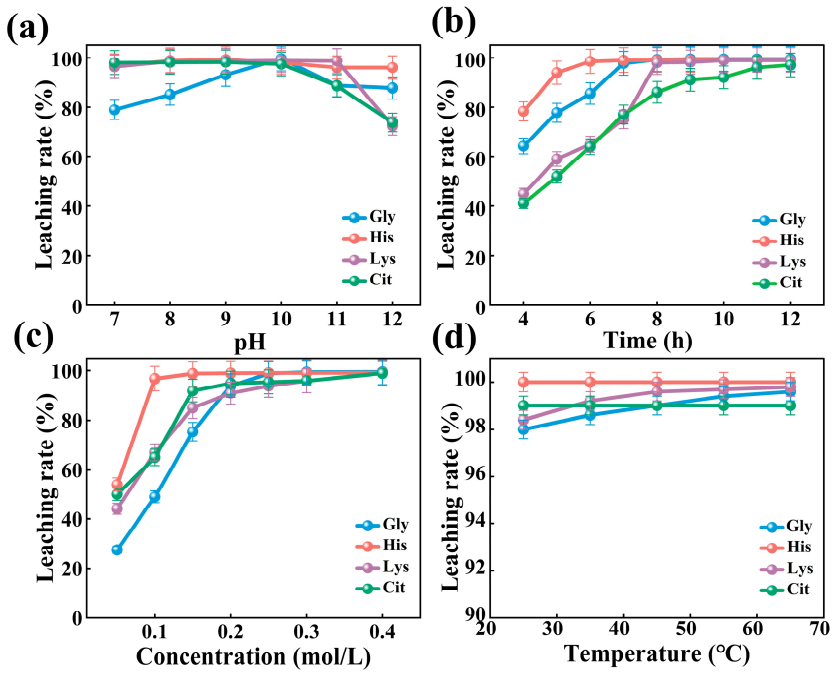


Figure 1. The leaching effects of different amino acids on cobalt varying with different pH (**a**), leaching time (**b**), amino acid concentrations (**c**), and leaching temperature (**d**).

The effect of leaching time on cobalt extraction efficiency of the above amino acids under suitable pH conditions is shown in Figure 1b. The experimental results indicated that the cobalt leaching rates of the four amino acids were different, among which histidine leached cobalt the fastest; all the cobalt was leached within 6 h. The order of the leaching rate was histidine, glycine, lysine, and citrulline. Therefore, the leaching times of histidine, glycine, lysine, and citrulline were set at 6, 7, 8, and 12 h, respectively, in the subsequent experiments.

Figure 1c shows that the rate of cobalt leaching increases with the increase in amino acid concentration. When the concentration of histidine was 0.1 mol/L, cobalt was completely leached. However, for other amino acids, the leaching rate of cobalt exceeds 90% only when their concentration is above 0.25 mol/L. Therefore, in subsequent experiments,

the concentration of histidine was set at 0.1 mol/L, while the concentration of other amino acids was set at 0.25 mol/L.

The results in Figure 1d indicate that temperature has a minimal effect on the leaching of cobalt by amino acids relative to other leaching parameters. In summary, under the conditions of 0.1 mol/L histidine concentration, a histidine/Co molar ratio of 1.8:1, room temperature, pH 8, and leaching for 6 h, the cobalt was completely leached. Thus, histidine is the best choice of amino acid for subsequent experiments.

3.2. Parameter Optimization

3.2.1. Effect of Temperature

The effect of leaching temperature on the extraction of cobalt using histidine is shown in Figure 2a. Leaching temperature has a significant impact on the leaching efficiency of cobalt. The higher the temperature, the faster the leaching rate. Under the conditions of 0.1 mol/L histidine concentration, a histidine/Co molar ratio of 1.8:1, and pH 8, the complete leaching of cobalt was achieved in 3 h at 55 °C. At 45 °C and 35 °C, complete leaching was achieved in 5 h. At room temperature, complete leaching was achieved in 6 h. Based on the Arrhenius equation (Equation (2)), the rate constant K relates to temperature. This phenomenon is attributed to the increase in the rate constant K of leaching reaction kinetics at higher temperatures, which accelerates the Brownian motion in cobalt powder, improves the diffusion and mass transfer efficiency within the leaching system, and thus promotes the leaching efficiency of cobalt. The leaching kinetics shown below prove this view. The temperature of 35 °C was chosen for the subsequent experiments, where the leaching rate of cobalt reached 99% at 6 h.

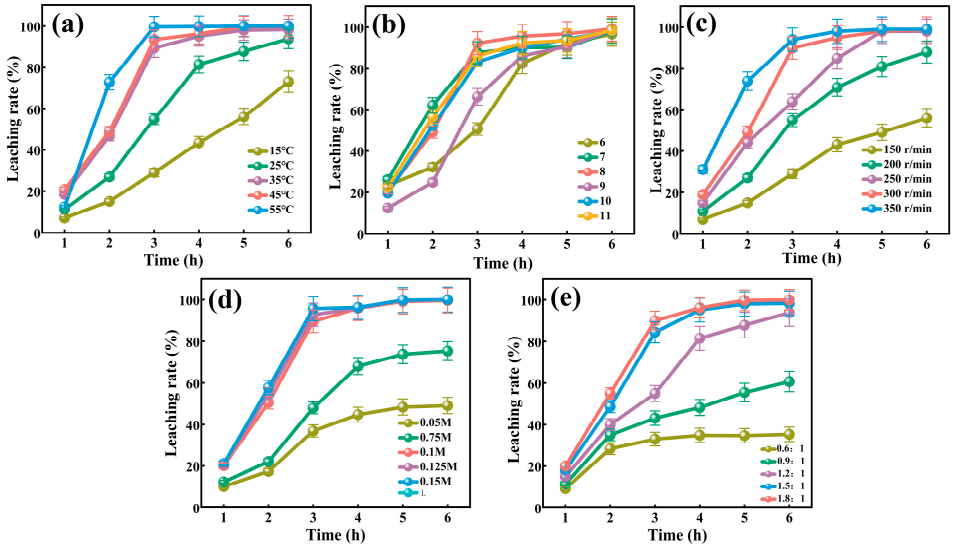


Figure 2. The effects of different factors on the extraction of cobalt using histidine: (**a**) temperature; (**b**) pH; (**c**) rotation speed; (**d**) histidine concentration; (**e**) molar ratio.

$$K = A \exp\left(-\frac{Ea}{RT}\right) \quad (2)$$

where K is the rate constant, in min^{-1}; A is the pre-exponential factor, dimensionless; Ea is the apparent activation energy of the reaction, in kJ mol^{-1}; R is the molar gas constant, 8.314 J/K mol; and T is the thermodynamic temperature in K.

3.2.2. Effect of pH

To investigate the leaching efficiency of cobalt using histidine at different pH values, the leaching kinetics of cobalt were examined under controlled conditions: a histidine concentration of 0.1 mol/L, a histidine/Co molar ratio of 1.8:1, a temperature of 35 °C, and a stirring speed of 300 rpm. As shown in Figure 2b, when the pH value is 8, the leaching rate of cobalt using histidine reaches up to 95% after 4 h. In general, as long as the leaching time is sufficient (extended to 6 h), cobalt can be completely leached under various pH (pH 6–11). This phenomenon can be attributed to the buffering capacity of the histidine solution leaching system, which consists of weak bases and acids, maintaining pH stability within a certain range, and thus ensuring a sustained high cobalt extraction rate.

3.2.3. Effect of Stirring Speed

The increase in stirring rate promotes the diffusion of oxygen and histidine in the leaching system, enhancing mass transfer between the liquid phases and cobalt powder, which in turn accelerates the leaching rate of cobalt. As shown in Figure 2c, the leaching rate of cobalt is positively correlated with stirring rates from 150 to 350 rpm. This phenomenon indicates that the stirring rate not only enhances the relative motion between the solid phase and the liquid phase (helping the leaving out of leach products, i.e., complexed cobalt ions) during the leaching process but also increases the concentration gradient of reactants in the liquid film, thereby accelerating diffusion and improving leaching efficiency. After considering both leaching efficiency and energy consumption, the stirring speed of 300 rpm was determined, at which the cobalt leaching rate reached 99%.

3.2.4. Effect of Histidine Concentration

Figure 2d indicates that the leaching efficiency of cobalt increased with histidine concentration (Figure 2d), rising from 53% at 0.05 mol/L to 99% at 0.1 mol/L after 4 h. This trend is attributed to the enhanced availability of histidine ligands, which drive the complexation equilibrium toward Co^{2+} dissolution. At concentrations exceeding 0.1 mol/L, leaching efficiency plateaued (>95% after 4 h), indicating a transition from ligand-limited to surface reaction-limited kinetics. As shown in Figure 1c, the superior efficiency of histidine over glycine (requiring $\geq$0.25 mol/L) underscores the critical role of its imidazole group in stabilizing Co^{2+} complexes. The leaching reaction can be represented as (Equation (3)):

$$Co^{2+} + nHis \rightarrow [Co(His)_n]^{2+} \quad (3)$$

3.2.5. Effect of His/Co Molar Ratio

The molar ratio of histidine to cobalt is crucial for improving the leaching efficiency of cobalt. The results shown in Figure 2e indicate that the leaching rate of cobalt increases with the amount of histidine. When the molar ratio was 1.5:1, the leaching rate of cobalt reached over 95%. However, further increasing the amount of histidine does not significantly improve the leaching rate of cobalt. Therefore, an excessively high molar ratio will instead increase the consumption of histidine. Thus, the molar ratio of histidine to cobalt was set at 1.5:1.

3.2.6. Selective Leaching of Cu-Co Alloy Slag

To determine the selective leaching effect of histidine on Cu-Co alloy slag, the leaching rates of Cu, Fe, Co, and Pb in a copper-cobalt alloy slag are shown in Figure 3a. The results indicate that the leaching rate of Co (88%) by histidine is significantly higher than that of Fe, Pb, and Cu. The effect of leaching time on histidine leaching of alloy slag is shown in Figure 3b. When the leaching time was 12 h, the leaching rate of Co reached 95%, while the leaching rates of Fe, Pb, and Cu were 0.7%, 1%, and 1%, respectively. When the leaching

time was extended to 24 h, the leaching rate of Co was further increased to 98%, while the leaching rates of other metals remain almost unchanged. The results demonstrate that the histidine leaching process has an excellent selective extraction effect on cobalt from alloy slag.

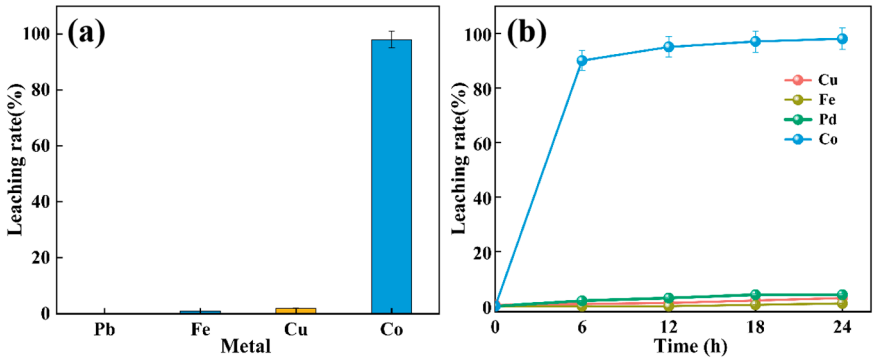


Figure 3. (**a**) Leaching rates of cobalt for 6 h at selective leaching (temperature 35 °C, histidine/cobalt molar ratio 1.5, pH 8); (**b**) Selective leaching of Co from Cu-Co alloy slag.

3.3. Characterization Analysis

The FT-IR spectra of the solid product from the leaching solution treated by freeze-drying (His-Co) and L-histidine are shown in Figure 4. The infrared spectrum of the histidine-cobalt sample showed significant differences compared to that of histidine. The positions of the main absorption peaks were obviously shifted and the intensity of the peaks changed, indicating a chemical reaction between histidine and cobalt. Compared with histidine, the N-H stretching vibration peak in His-Co was red-shifted, i.e., the frequency decreased from 1475 cm^{-1} to 1464 cm^{-1}, indicating the weakening of the N-H bond strength and the complexation reaction between the amino group and Co^{2+} ions. The symmetric stretching vibration peak of COO- shifted from 1437 cm^{-1} to 1414 cm^{-1}, which is due to the complexing of COO- with Co^{2+} ions, resulting in a decrease in the electron cloud density of the COO- group. The COOH absorption peak at 1633 cm^{-1} narrows significantly, which is attributed to the weakening of intermolecular or intramolecular interactions, resulting in an increase in the degree of freedom of the molecule, and the vibration frequency is concentrated as a narrowing of the peak [26]. However, the peak at 1586 cm^{-1} corresponds to the asymmetric CC bond stretching vibration of the imidazole ring [27], which is not present in the infrared spectrum of L-histidine. Furthermore, new characteristic peaks appeared in the spectrum of His-Co at 1343 cm^{-1}, 1250 cm^{-1}, and 923 cm^{-1}, which corresponded to the asymmetric stretching absorption peaks of NH^{3+}, C-N, C-N/N-H, and C-H, respectively [28–30]. The asymmetric stretching vibration peak of C-N shifted from 1114 cm^{-1} to 1084 cm^{-1}, further confirming the involvement of the amino group in the reaction [31]. It is noteworthy that the strong absorption peak at 625 cm^{-1} originates from the vibration of the imidazole ring. The Co-N vibration peak at 539 cm^{-1} directly reveals the coordination relationship between the amino group and the cobalt ion. Based on FT-IR analysis, it is speculated that the amino group and COO- group in histidine played a complexing role in the cobalt leaching reaction.

Figure 5a presents the comprehensive XPS spectrum of the main elements in the leaching solution. To compare the peak binding energies of the elements in leaching solution to those of standard spectra, the analysis results are shown in Figure 5b–e. Figure 5b illustrates the C1s spectrum with three peaks at 284.8 eV, 285.79 eV, and 288.07 eV, corresponding to the orbital binding energies of C1s in sp_2- or sp_3-hybridized C-H or C-C bonds [32,33], the C=N in the imidazole group of histidine, and the C=O bond [34]. In Figure 5c, N1s peaks at 398.4 eV and 399.5 eV are attributed to C=N and CO-NH_2, respectively. Figure 5d

shows that the O1s peaks of the main oxygen-containing groups are located at 530.8 eV and 532.5 eV, which belong to the bands of O-C-O and CoO [35], respectively. The content of O-C-O is dominant, indicating that there was still unreacted histidine in the leaching solution. The peaks of 802 eV and 796.1 eV shown in Figure 5e correspond to the Co $2p_{1/2}$ orbital characteristic peaks of CoO and Co^{2+}, respectively, while the peaks of 785.6 eV and 780.6 eV represent the Co $2p_{3/2}$ orbital characteristic peaks of CoO and Co^{2+} [36]. The coexistence of O1s and Co2p peaks for CoO indicates the bonding of O atoms with Co ions. Based on these analyses, it is concluded that metallic Co was leached as Co^{2+} during the process. Considering the orbital binding energies of Co and C/O/N atoms in functional groups, it is inferred that electrons were donated to Co^{2+} by the amino and carboxyl groups of histidine during coordination. This finding is consistent with the XPS peak of Co^{2+} (796.1 eV), which match the reported values for Co-histidine complexes, confirming the formation of $[Co(His)_2]^{2+}$. Additionally, the FT-IR results (N-H shift from 1475 to 1464 cm^{-1}) further support the proposed coordination mechanism via amino and carboxyl groups.

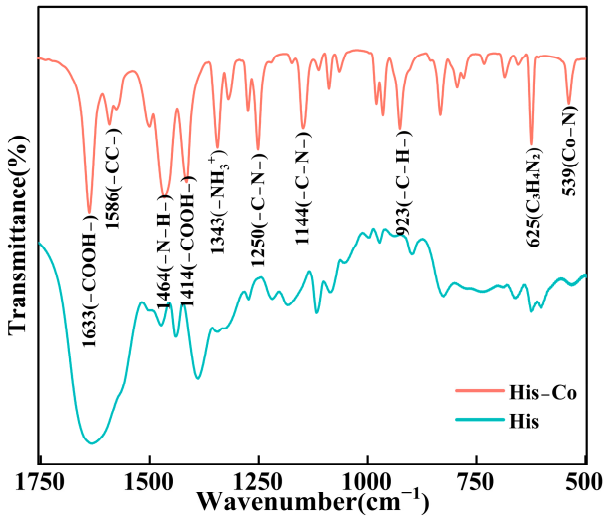


Figure 4. FT-IR of histidine and the solid product from the leaching solution treated by freeze-drying.

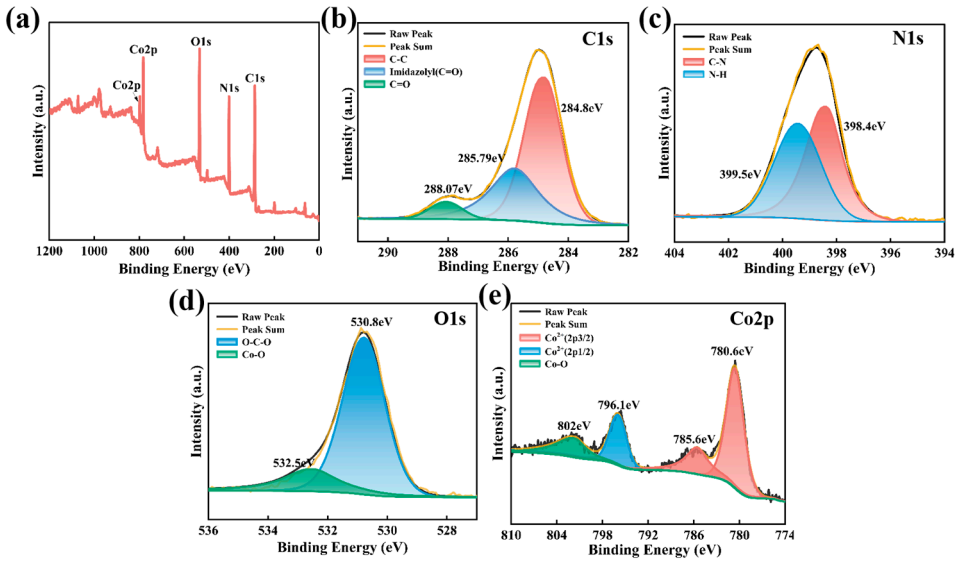


Figure 5. XPS spectra of the solid product from the leaching solution treated by freeze-drying. (**a**) XPS survey spectrum after leaching; (**b**–**e**) XPS spectra after leaching.

As shown in Figure 6a,b, the SEM analyses revealed the surface morphology characteristics of the original cobalt powder and the solid product from the leaching solution treated by freeze-drying. Compared with the irregular strip morphology of the original cobalt powder, the cobalt surface after reaction with histidine exhibits the phenomenon of leaching corrosion. Figure 6c shows the EDS analysis of the solid product from the leaching solution treated by freeze-drying; the content ratios of elements such as C, H, O, and Co were very close to those of $Co(C_6H_9N_3O_2)_2$. Combined with the previous FT-IR and XPS analyses, it was verified that O-C-O and -NH- in histidine formed metal ligands with cobalt ions. The mechanism of cobalt leaching by using histidine could be described as shown in Figure 7.

3.4. Leaching Kinetics

To describe the reaction kinetics mechanism of cobalt leaching using histidine, the film diffusion model (Equation (4)), the chemical reaction control model (Equation (5)), the product layer diffusion control model (Equation (6)), and mixing control model (Equation (7)) are used and fitted to identify the leaching process rate-controlling step [37,38].

$$X = kt \tag{4}$$

$$1 - (1 - X)^{\frac{1}{3}} = kt \tag{5}$$

$$1 - \frac{2}{3}X - (1 - X)^{\frac{2}{3}} = kt \tag{6}$$

$$\frac{1}{3}\ln(1 - X) + (1 - X)^{\frac{-1}{3}} - 1 = kt \tag{7}$$

where X is the leaching rate of metal, t is the leaching time (h), and k is the constant of apparent rate.

As illustrated in Figure 8 and Table 2, the fitting coefficient (R_2) of the equation of the surface chemical reaction control model exceeds 0.98 at different temperatures, indicating that the surface chemical reaction control model has a good linear relationship with the cobalt powder leaching time and is significantly higher than the correlation coefficient obtained by the fitting of the internal diffusion control and mixing control of the solid product layer. Therefore, it is preliminarily believed that the histidine leaching process was controlled by surface chemical reactions, which is further confirmed by the calculation of the activation energy of the reaction. The apparent activation energy for the leaching reaction was calculated using the Arrhenius equation, the results for which are shown in Figure 9. It is widely acknowledged that the apparent activation energy (Ea) is less than 12.5 kJ/mol, indicating that the leaching process is diffusion-controlled in the product layer. If 12 < Ea < 41.8 kJ/mol, the leaching process is a mixed-controlled process. When Ea > 41.8 kJ/mol, the leaching process is a chemical reaction-controlled process [39].

The results shown in Figure 9 and Table 3 demonstrate that the surface chemical control kinetic model at different temperatures has a good fitting effect; the correlation coefficient (R_2) was 0.99. The apparent activation energy (Ea) for the cobalt leaching process was 64.32 kJ/mol, which was consistent with the activation energy Ea > 41.8 kJ/mol, indicating that the cobalt leaching process mainly conformed to the surface chemical control model and was consistent with the results obtained by fitting the kinetic model (Table 2).

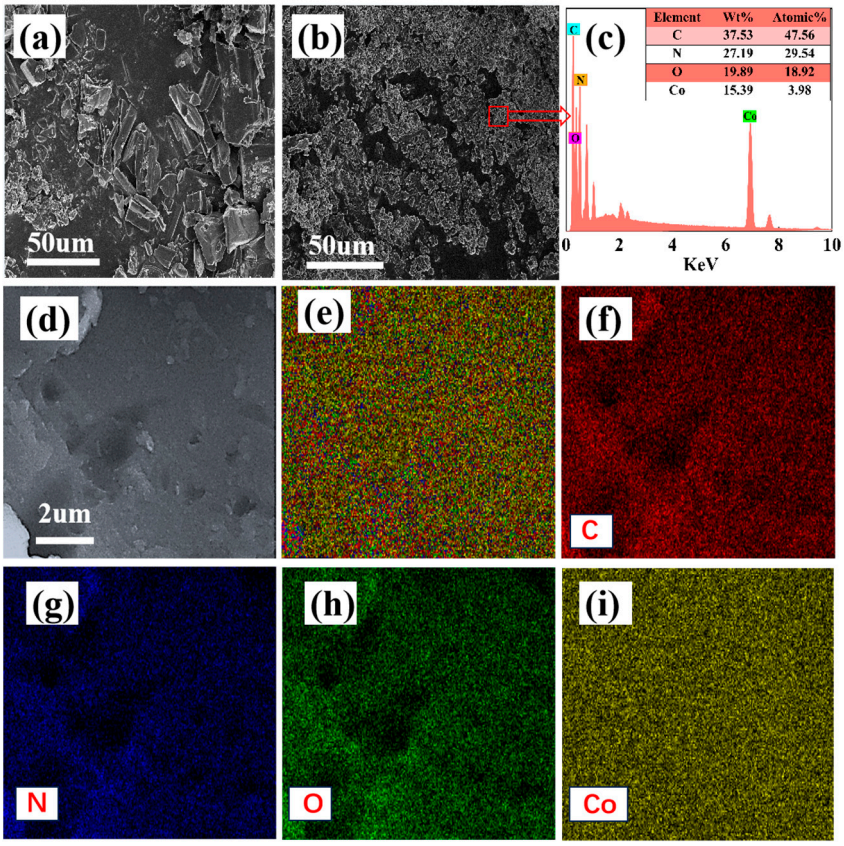


Figure 6. SEM-EDS analyses of cobalt powder (**a**) and the solid product from the leaching solution treated by freeze-drying (**b**–**i**).

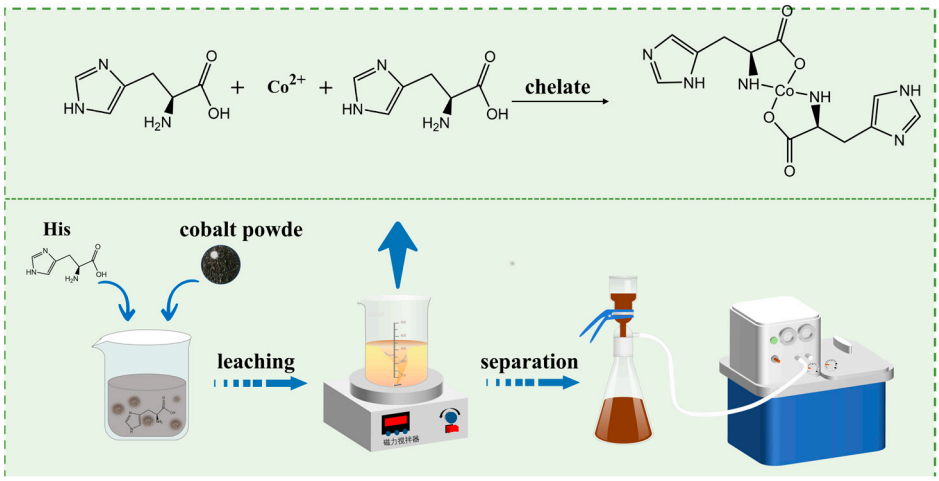


Figure 7. The mechanism of cobalt leaching using histidine.

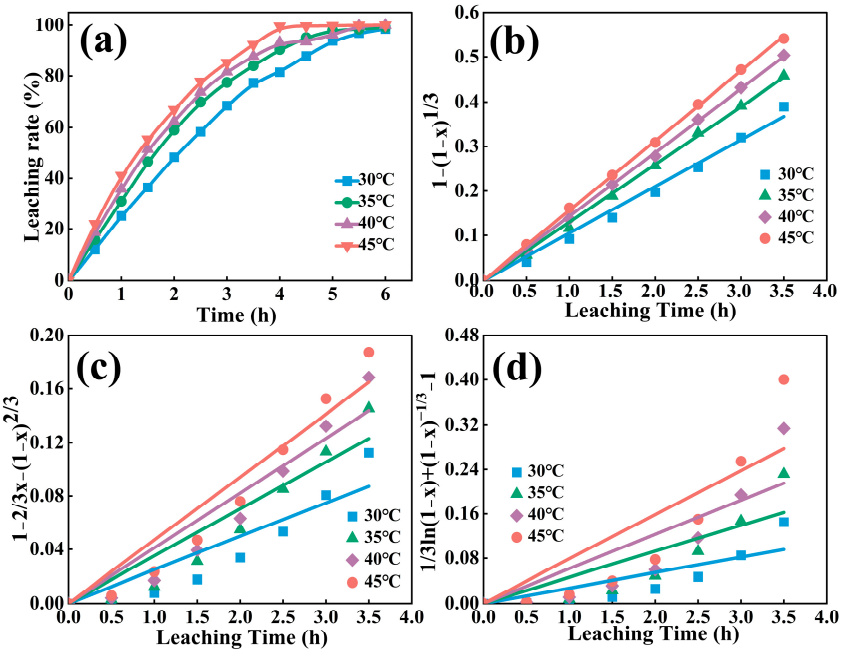


Figure 8. (**a**) The effect of temperature on copper leaching rate; fitting curves of leaching rate with three kinetics equations: (**b**) chemical reaction; (**c**) internal diffusion; and (**d**) mixed control model.

Table 2. Fitting parameters of the equations for the three kinetic models for cobalt leaching using histidine.

Temperature (°C)	Internal Diffusion Control $1-(2/3)x-(1-x)^{2/3}$		Chemical Reaction Control $1-(1-x)^{1/3}$		Mixed Control $1/3\ln(1-x)+(1-x)^{-1/3}-1$	
	k_1 (min^{-1})	R_2	k_2 (min^{-1})	R_2	k_2 (min^{-1})	R_2
30	0.02493	0.846	0.05406	0.989	0.02732	0.716
35	0.03519	0.902	0.08991	0.998	0.04637	0.765
40	0.04110	0.911	0.13334	0.999	0.06148	0.747
45	0.04709	0.929	0.17980	0.999	0.07924	0.752

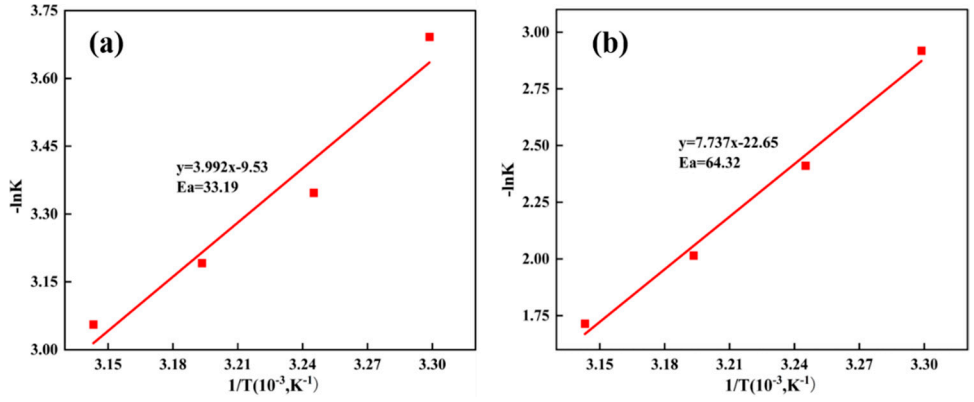


Figure 9. Arrhenius plots for (**a**) internal diffusion and (**b**) chemical reaction at different temperatures.

Table 3. The activation energy of the two control models.

Control Model	Slope k′	Correlation Coefficient (R_2)	Ea (kJ/mol)
Chemical reaction control	7.74	0.99	64.32
Internal diffusion control	3.99	0.95	33.19

A nucleation model based on the ideal sphere hypothesis is proposed to simulate the leaching process of solid particles. According to the model, the main chemical reaction occurs between the unreacted particle core and the surface of the phase boundary of the reaction product [40]. The leaching process occurs isotropically from the outer surface towards the interior of the spherical particles, preserving the core's spherical configuration, as illustrated in Figure 10. The leaching steps mainly include the following: I. The leaching agent diffuses towards the surface of the cobalt powder; II. The leaching agent diffuses inward through the solid film; III. The leaching agent reacts with cobalt powder; IV. The product (Co-histidine complex) diffuses out of the reaction site; V. The product finally enters the solution through the diffusion layer [41].

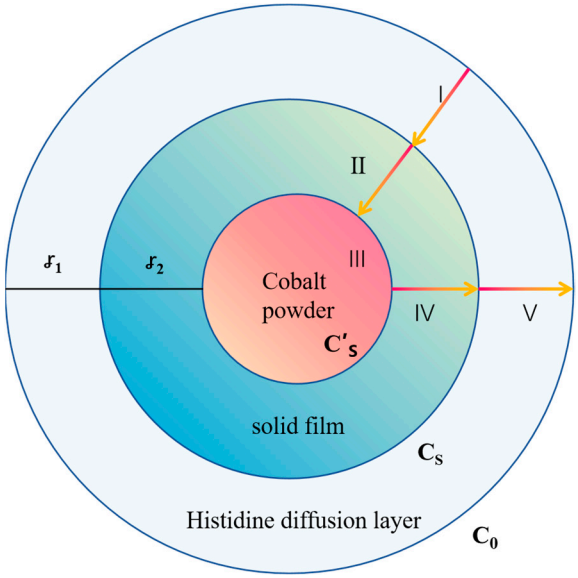


Figure 10. Diagram of the process for leaching cobalt powder with histidine (C_0: leaching agent concentration in water, C_S: leaching agent concentration on the solid surface, C'_S: leaching agent concentration in the reaction zone, δ_1: effective thickness of the leaching agent diffusion layer, δ_2: solid film thickness).

3.5. Future Research Prospects

This study demonstrates that histidine-mediated selective leaching of cobalt is technically feasible. However, additional rigorous laboratory experiments are required before scaling up this technology for industrial or commercial applications. In practical leaching operations, recovery and recycling of the leaching solution should be implemented to reduce operational costs. Furthermore, potential synergies with existing hydrometallurgical technologies could be explored, such as combining histidine leaching with electrochemical processes or solvent extraction techniques. The results reveal relatively low nickel leaching efficiency by histidine (only 1% after 24 h). Future research could focus on optimizing leaching parameters (e.g., pH adjustment, redox agents) or incorporating histidine with auxiliary ligands like glycine to enhance nickel selectivity. Concurrently, conducting a life cycle assessment (LCA) to compare the environmental footprint of histidine leaching with conventional ammonia-based or acid-based methods would help evaluate the viability of histidine leaching as a versatile and sustainable alternative in hydrometallurgical processes.

4. Conclusions

The recovery of cobalt was efficiently achieved through a selective complexation leaching method utilizing histidine as a green leaching agent. Compared to glycine-based systems, histidine was demonstrated to rapidly form stable soluble complexes with Co^{2+}

at lower concentrations across a broader alkaline pH range (6–11). In this study, histidine was innovatively introduced as a sustainable alternative to glycine for cobalt recovery, exhibiting significantly accelerated leaching kinetics and enhanced pH adaptability. The leaching process exhibited high selectivity toward cobalt. Under optimized conditions (initial pH 8, 35 °C, 0.1 mol/L histidine concentration, 300 rpm stirring speed, histidine/Co molar ratio of 1.5:1, and 12 h duration), extraction efficiencies of 95% Co, 0.7% Fe, 1% Pb, and 1% Cu were attained. Kinetic analysis revealed that cobalt extraction was governed by surface chemical reactions, with an activation energy of 64.32 kJ/mol. The coordination mechanism was confirmed through FT-IR and XPS analyses, which indicated that Co^{2+} in solution predominantly interacted with the -O=C-O- and -N-H functional groups of histidine, leading to the formation of stable chelate ring complexes. This study successfully validated the feasibility of employing histidine as a highly efficient and selective leaching agent for cobalt separation from cobalt-rich alloy slags.

Author Contributions: Conceptualization, W.G. and Y.Z. (Yaolong Zhang); methodology, X.Z. (Xi ankun Zhou); data curation, X.Z. (Xu Zhao); writing—original draft preparation, M.L.; writing—review and editing, Z.L. and Y.Z. (Yahui Zhang); supervision, Q.W. All authors have read and agreed to the published version of the manuscript.

Funding: This research was funded by the Research Project of Hunan Provincial Education Department of China, grant number 22B0440 and Hunan Students' platform for innovation and entrepreneurship training program (S202310555017 and S202210555346).

Data Availability Statement: The original contributions presented in this study are included in the article. Further inquiries can be directed to the corresponding authors.

Conflicts of Interest: The authors declare that they have no known competing financial interests or personal relationships that could have appeared to influence the work reported in this paper.

References

1. Oke, E.A.; Potgieter, H.; Mondlane, F.; Skosana, N.P.; Teimouri, S.; Nyembwe, J.K. Concurrent leaching of copper and cobalt from a copper-cobalt ore using sulfuric and organic acids. *Miner. Eng.* **2024**, *216*, 108853. [CrossRef]
2. Zhang, L.; Xiao, W.; Li, G.; Wang, D.; Wu, J.; Du, H.; Lin, Y.; Ye, C.; Qi, T.; Wang, Z. A cleaner and sustainable method for recovering rare earth and cobalt from NdFeB leaching residues. *J. Clean. Prod.* **2023**, *422*, 138576.
3. Huang, Y.; Chen, P.; Shu, X.; Fu, B.; Peng, W.; Liu, J.; Cao, Y.; Zhu, X. Extraction and recycling technologies of cobalt from primary and secondary resources: A comprehensive review. *Int. J. Miner. Metall. Mater.* **2024**, *31*, 628–649.
4. Qin, H.; Makuza, B.; Zhao, J.; Yu, D.; Guo, X.; Tian, Q. Hydrochlorination of Copper-Cobalt Alloy for Efficient Separation of Valuable Metals. *J. Sustain. Metall.* **2022**, *8*, 795–805.
5. Jung, H.; Inaba, Y.; Jiang, V.; West, A.C.; Banta, S. Engineering Polyhistidine Tags on Surface Proteins of Acidithiobacillus ferrooxidans: Impact of Localization on the Binding and Recovery of Divalent Metal Cations. *ACS Appl. Mater. Interfaces* **2022**, *14*, 10125–10133. [CrossRef]
6. Cai, C.; Fajar, A.T.; Hanada, T.; Wakabayashi, R.; Goto, M. Amino Acid Leaching of Critical Metals from Spent Lithium-Ion Batteries Followed by Selective Recovery of Cobalt Using Aqueous Biphasic System. *ACS Omega* **2023**, *8*, 3198–3206. [PubMed]
7. Lin, L.; Lu, Z.; Zhang, W. Recovery of lithium and cobalt from spent Lithium- Ion batteries using organic aqua regia (OAR): Assessment of leaching kinetics and global warming potentials. *Resour. Conserv. Recycl.* **2021**, *167*, 105416.
8. Tian, L.; Gong, A.; Wu, X.; Yu, X.; Xu, Z.; Chen, L. Process and kinetics of the selective extraction of cobalt from high-silicon low-grade cobalt ores using ammonia leaching. *Int. J. Miner. Metall. Mater.* **2022**, *29*, 218–227.
9. Biswal, B.K.; Jadhav, U.U.; Madhaiyan, M.; Ji, L.; Yang, E.H.; Cao, B. Biological Leaching and Chemical Precipitation Methods for Recovery of Co and Li from Spent Lithium-Ion Batteries. *ACS Sustain. Chem. Eng.* **2018**, *6*, 12343–12352.
10. Li, L.; Bian, Y.; Zhang, X.; Guan, Y.; Fan, E.; Wu, F.; Chen, R. Process for recycling mixed-cathode materials from spent lithium-ion batteries and kinetics of leaching. *Waste Manag.* **2018**, *71*, 362–371. [CrossRef]
11. Oraby, E.; Deng, Z.; Li, H.; Eksteen, J. Selective extraction of nickel and cobalt from disseminated sulfide flotation cleaner tailings using alkaline glycine-ammonia leaching solutions. *Miner. Eng.* **2023**, *204*, 108418. [CrossRef]
12. Shi, S.X.; Jiang, S.Q.; Nie, C.C.; Li, B.; Chang, H.H.; Zhu, X.N. Kinetic characteristics and mechanism of copper leaching from waste printed circuit boards by environmental friendly leaching system. *Process Saf. Environ. Prot.* **2022**, *166*, 123–132. [CrossRef]

13. Oraby, E.; Li, H.; Deng, Z.; Eksteen, J. Selective extraction of Ni and Co from a pyrrhotite-rich flotation slime using an alkaline glycine-based leach system. *Miner. Eng.* **2023**, *203*, 108330. [CrossRef]
14. Oraby, E.; Eksteen, J. The selective leaching of copper from a gold–copper concentrate in glycine solutions. *Hydrometallurgy* **2014**, *150*, 14–19. [CrossRef]
15. Chen, M.; Wang, R.; Qi, Y.; Han, Y.; Wang, R.; Fu, J.; Meng, F.; Yi, X.; Huang, J.; Shu, J. Cobalt and lithium leaching from waste lithium ion batteries by glycine. *J. Power Sources* **2021**, *482*, 228942. [CrossRef]
16. Sethurajan, M.; Shirodker, M.G.P.; Rene, E.R.; van Hullebusch, E.D. Hydrometallurgical leaching and recovery of cobalt from lithium ion battery. *Environ. Technol. Innov.* **2022**, *28*, 102915. [CrossRef]
17. Eksteen, J.; Oraby, E.; Nguyen, V. Leaching and ion exchange based recovery of nickel and cobalt from a low grade, serpentine-rich sulfide ore using an alkaline glycine lixiviant system. *Miner. Eng.* **2020**, *145*, 106073. [CrossRef]
18. Li, H.; Deng, Z.; Oraby, E.; Eksteen, J. Amino acids as lixiviants for metals extraction from natural and secondary resources with emphasis on glycine: A literature review. *Hydrometallurgy* **2023**, *216*, 106008. [CrossRef]
19. Sun, Y.; Shi, Y.; Li, C.; Shi, H. Histidine Protonation Behaviors on Structural Properties and Aggregation Properties of Aβ(1-42) Mature Fibril: Approaching by Edge Effects. *J. Phys. Chem.* **2024**, *128*, 7341–7349. [CrossRef]
20. Essential Amino Acids. Findings from University Erlangen-Nurnberg Has Provided New Data on Essential Amino Acids (A facile UV-light mediated synthesis of L-histidine stabilized silver nanocluster for efficient photodegradation of methylene blue). *Sci. Lett.* **2015**, *404*, 27–35.
21. Li, H.; Oraby, E.; Eksteen, J. An alternative amino acid leaching of base metals from waste printed circuit boards using alkaline glutamate solutions: A comparative study with glycine. *Sep. Purif. Technol.* **2025**, *356*, 129953.
22. Liu, Z.; Zu, Y.; Fu, Y.; Meng, R.; Guo, S.; Xing, Z.; Tan, S. Hydrothermal synthesis of histidine-functionalized single-crystalline gold nanoparticles and their pH-dependent UV absorption characteristic. *Colloids Surf. B Biointerfaces* **2009**, *76*, 311–316. [CrossRef] [PubMed]
23. Nidya, M.; Umadevi, M.; Rajkumar, B.J. Optical and morphological studies of L-histidine functionalised silver nanoparticles synthesised by two different methods. *J. Exp. Nanosci.* **2015**, *10*, 167–180.
24. Lin, S.M.; Geng, S.; Li, N.; Liu, S.G.; Li, N.B.; Luo, H.Q. l-Histidine-protected copper nanoparticles as a fluorescent probe for sensing ferric ions. *Sens. Actuators B. Chem.* **2017**, *252*, 912–918.
25. Eksteen, J.; Oraby, E. The leaching and adsorption of gold using low concentration amino acids and hydrogen peroxide: Effect of catalytic ions, sulphide minerals and amino acid type. *Miner. Eng.* **2015**, *70*, 36–42. [CrossRef]
26. Armentrout, P.B.; Stevenson, B.C.; Ghiassee, M.; Boles, G.C.; Berden, G.; Oomens, J. Infrared multiple-photon dissociation spectroscopy of cationized glycine: Effects of alkali metal cation size on gas-phase conformation. *Phys. Chem. Chem. Phys.* **2022**, *24*, 37.
27. Lei, T.; Shu, J.; Deng, Y.; Hu, L.; Chen, S.; Chen, M.; Huang, W. Enhanced recovery of copper from reclaimed copper smelting fly ash via leaching and electrowinning processes. *Sep. Purif. Technol.* **2021**, *273*, 118943.
28. Boukaoud, A.; Chiba, Y.; Sebbar, D. A periodic DFT study of IR spectra of amino acids: An approach toward a better understanding of the N-H and O-H stretching regions. *Vib. Spectrosc.* **2021**, *116*, 103280.
29. Pyreu, D.; Gridchin, S. Mixed-Ligand Nickel(II) Complexes with Histidine and Cysteine in Aqueous Solution: Thermodynamic Approach. *J. Solut. Chem.* **2023**, *53*, 372–385.
30. Tian, H.; Guo, Z.; Pan, J.; Zhu, D.; Yang, C.; Xue, Y.; Li, S.; Wang, D. Comprehensive review on metallurgical recycling and cleaning of copper slag. *Resour. Conserv. Recycl.* **2021**, *168*, 105366. [CrossRef]
31. Paiva, F.; Batista, J.; Rêgo, F.; Lima, J.; Freire, P.; Melo, F.; Filho, J.M.; de Menezes, A.; Nogueira, C. Infrared and Raman spectroscopy and DFT calculations of DL amino acids: Valine and lysine hydrochloride. *J. Mol. Struct.* **2017**, *1127*, 419–426.
32. Haripriya, M.; Manimekala, T.; Dharmalingam, G.; Minakshi, M.; Sivasubramanian, R.J.C.A.A.J. Asymmetric Supercapacitors Based on $ZnCo_2O_4$ Nanohexagons and Orange Peel Derived Porous Carbon Electrodes. *Chem. Asian J.* **2024**, *19*, e202400202. [PubMed]
33. Ayyanusamy, P.; Alphonse, R.; Minakshi, M.; Sivasubramanian, R. Synthesis of amorphous nickel-cobalt hydroxides for Ni-Zn rechargeable aqueous battery. *Chemistry* **2024**, *30*, e202402325. [CrossRef]
34. Amino Acids-Histidine. New Histidine Findings from University of Tanta Reported (Nano-sized metal complexes of azo L-histidine: Synthesis, characterization and their application for catalytic oxidation of 2-amino phenol). *Chem. Chem.* **2018**, *32*, 4229.
35. Amino Acids-Histidine. Findings from Y. He and Colleagues Update Understanding of Histidine (Histidine and histidine dimer as green inhibitors for carbon steel in 3wt% sodium chloride solution; Electrochemical, XPS and Quantum chemical calculation studies). *J. Eng.* **2018**, *13*, 2136–2153.
36. Technology—Vacuum Technology. Study Findings from D. Moszynski et al. Broaden Understanding of Vacuum Technology (XPS study of cobalt-ceria catalysts for ammonia synthesis—The reduction process). *Chem. Chem.* **2018**, *155*, 434–438.

37. Han, Y.; Yi, X.; Wang, R.; Huang, J.; Chen, M.; Sun, Z.; Sun, S.; Shu, J. Copper extraction from waste printed circuit boards by glycine. *Sep. Purif. Technol.* **2020**, *253*, 117463.
38. Hosseinzadeh, M.; Entezari Zarandi, A.; Pasquier, L.C.; Azizi, A. Kinetic Investigation on Leaching of Copper from a Low-Grade Copper Oxide Deposit in Sulfuric Acid Solution: A Case Study of the Crushing Circuit Reject of a Copper Heap Leaching Plant. *J. Sustain. Metall.* **2021**, *7*, 1154–1168.
39. Bidari, E.; Aghazadeh, V. Investigation of Copper Ammonia Leaching from Smelter Slags: Characterization, Leaching and Kinetics. *Metall. Mater. Trans.* **2015**, *46*, 2305–2314.
40. Tanda, B.C.; Oraby, E.A.; Eksteen, J.J. Kinetics of malachite leaching in alkaline glycine solutions. *Miner. Process. Extr. Metall.* **2021**, *130*, 16–24.
41. Apua, M.C.; Madiba, M.S. Leaching kinetics and predictive models for elements extraction from copper oxide ore in sulphuric acid. *J. Taiwan Inst. Chem. Eng.* **2021**, *121*, 313–320. [CrossRef]

Disclaimer/Publisher's Note: The statements, opinions and data contained in all publications are solely those of the individual author(s) and contributor(s) and not of MDPI and/or the editor(s). MDPI and/or the editor(s) disclaim responsibility for any injury to people or property resulting from any ideas, methods, instructions or products referred to in the content.